IEEE Photonics Journal
An IEEE Photonics Society Publication

Irrotational Nanobricks Based High-Efficiency Polarization-Independence Metasurfaces

Volume 12, Number 4, August 2020

Wei Wang
Zehan Zhao
Chong Guo
Fei Shen
Jinghua Sun
Zhongyi Guo

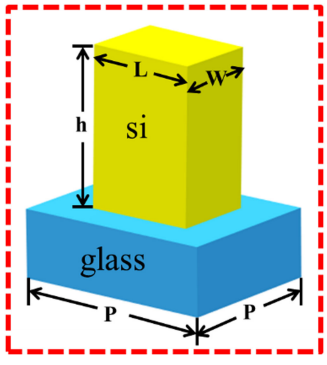

DOI: 10.1109/JPHOT.2020.3002692

Irrotational Nanobricks Based High-Efficiency Polarization-Independence Metasurfaces

Wei Wang,[1,2] Zehan Zhao,[1] Chong Guo,[1] Fei Shen,[2] Jinghua Sun,[2] and Zhongyi Guo [2,3]

[1]Department of Mathematics and Physics, Shijiazhuang Tiedao University, Shijiazhuang 050043, China
[2]School of Electrical Engineering and Intelligentization, Dongguan University of Technology, Dongguan 523808, China
[3]School of Computer and Information, Hefei University of Technology, Hefei 230009, China

DOI:10.1109/JPHOT.2020.3002692

Manuscript received April 15, 2020; revised June 10, 2020; accepted June 12, 2020. Date of publication June 16, 2020; date of current version July 14, 2020. This work was supported in part by the National Natural Science Foundation of China under Grants 11704265 and 61775050, in part by Natural Science Foundation of Hebei Province, China under Grant A2019210050, and in part by Youth Top Talent Program of Hebei Provincial Department of Education, China under Grant BJ2018033. Corresponding author: Zhongyi Guo (e-mail: guozhongyi@hfut.edu.cn).

Abstract: The polarization-independence optical metasurface has attracted great interests due to breaking the polarization limitations. In general, polarization-independence characteristics of metasurface almost always originates from the polarization-independence characteristics of the used resonant antenna itself. In this paper, a novel approach is proposed to achieve polarization-independence metasurface based on the irrotational nanobricks. Firstly, the intrinsic characteristics of a half wave plate has been investigated, which can realize co-polarization transmission of X-linear-polarization (XLP) and Y-linear-polarization (YLP) lights, and cross-polarization transmission of circular polarization (CP) light, simultaneously. Eight high-efficiency silicon nanobricks with the phase shifts over 2π are designed as the basic unit cell, which have the same transmitted amplitude and phase for the CP and XLP light, and the phase difference for XLP and YLP light. We have also designed the beam deflector, metalens and vortex beam generator, which possess identical function for cross-polarized CP and co-polarized XLP and YLP light, respectively. These results can promote the deeper understanding of metasurface, and give a new method to design polarization-independent optical devices.

Index Terms: Metasurface, spin, phase modulation, polarization-independence.

1. Introduction

Optical metasurfaces, a two-dimensional planar metamaterials, have been successfully designed to achieve unusual electromagnetic properties, which can arbitrarily manipulate wavefront by controlling the amplitude, phase, and polarization of output light [1]–[3]. The metasurface is generally composed of nano-antennas or meta-atoms which can bring forth arbitrary abrupt phase shifts by changing geometric shape, sizes or materials. Different from the conventional optical devices, metasurface optical devices possess ultrathin, low-cost, highly integrated characteristics, which will promote the development of nano-optoelectronics and microdevices. The initial metasurface optical devices consist of metal nanoantennas, and they suffer from low efficiency due to the ohmic

losses [4]–[8]. For achieving high transmission efficiency, reflective metasurfaces [9] and dielectric metasurfaces [10]–[12] have gained significant attentions in recent years. Dielectric metasurfaces are made from high refractive index materials, by which various optical components with high transmission efficiency have been demonstrated, including beam shapers [13], [14], metalenses [15], [16], holograms [17], [18], optical vortex generators [19], [20], chiral metasurface [21], [22] and achiral metasurface [23]–[26].

Although the metasurfaces can achieve the control of light at sub-wavelength scales, there is still a big challenge for some practical applications of metasurfaces due to their polarization-dependence for incident circularly polarized (CP) light. As far as we know, the polarization states of CP light can also be manipulated by the metasurfaces, which are closely related to the Pancharatnam-Berry (PB) phase, and the sign of PB phase is jointly decided by the sign of the orientation angle of the basic nanoantennas and the polarization states of the incident circularly polarized light [27], [28]. Various optical devices of metasurface based on PB phase are designed, such as, dual-polarity metalens [29]–[31] spin-dependent beam splitters [32], vortex phase plate [33], [34], holograms [35], [36] and so on. These metasurface devices possess different functions for left-handed circularly polarized (LCP) and right-handed circularly polarized (RCP) incidences. Recently, some polarization-independent metasurface have been reported, and they are all composed of elements with rotational invariance or with the symmetrical axis's orientation angle of 45° or 135° [37]–[41]. And the spin-independent metalens composed of two polarity-inverse multiplexing metalenses with the same focal length have also been reported [16], [42]. However, to our knowledge, the spin-independent metasurfaces composed of spin-independent nanobricks without rotation have not been proposed and investigated before, and the polarization-independent metasurfaces composed of polarization-dependent nanobricks without rotation also have not attracted people's attention before.

In this paper, a series of novel polarization-independent metasurface have been proposed for linear polarized (LP) and CP incident lights, which is constructed by silicon nanobricks as half wave plate. These ingenious silicon nanobricks possess the same transmitted amplitude and phase for CP and X-linear polarized (XLP) light, the phase difference is for XLP and Y-linear polarized (YLP) incident lights, so, the metasurface possesses the co-polarized and cross-polarized transmission function for LP and CP incidences, respectively. And the phase variation from 0 to 2π is determined just by the lengths of two arms of the silicon nanobricks instead of conventional rotation of the nanostructures. A detailed theoretical analysis based on the Jones matrix and the numerical simulations are employed to confirm the polarization-independence of the metasurface and the intrinsic characteristics of a half wave plate (HWP). The polarization-independent beam deflector, metalens and vortex beam generator are designed based on eight nanobricks, which can achieve identical function for CP and LP incidences. Our design breaks people's cognition that the metasurface applicable to CP light depends on PB phase, and also breaks the cognition that the metasurface with polarization independence will have certain symmetry.

2. Design and Analysis

As everyone knows, the relation in the linear-polarization bases between the incident (E^i) and transmitted (E^t) electromagnetic waves can be described using the Jones matrix:

$$\begin{bmatrix} E_x^t \\ E_y^t \end{bmatrix} = T \cdot \begin{bmatrix} E_x^i \\ E_y^i \end{bmatrix} \text{ where, } T = \begin{bmatrix} T_{xx} & T_{xy} \\ T_{yx} & T_{yy} \end{bmatrix} \tag{1}$$

And, in the circular-polarization base, the relationship between incident and transmitted electromagnetic waves can be expressed by the transformation matrix S:

$$\begin{bmatrix} E_L^t \\ E_R^t \end{bmatrix} = STS^{-1} \begin{bmatrix} E_L^i \\ E_R^i \end{bmatrix} \tag{2}$$

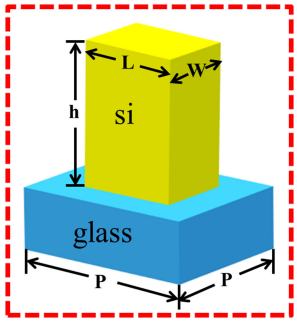

Fig. 1. Schematic of the Si nanobrick.

There is a conversion relationship [41]:

$$\begin{bmatrix} E_L \\ E_R \end{bmatrix} = S \cdot \begin{bmatrix} E_x \\ E_y \end{bmatrix} \quad \text{and } S = \frac{\sqrt{2}}{2} \begin{bmatrix} 1 & -i \\ 1 & i \end{bmatrix} \tag{3}$$

And, the transmitted electric field for incidences with any polarization states can be reduced to $E = \begin{bmatrix} E_x \\ E_y e^{i\varphi} \end{bmatrix}$, where$\varphi$is the phase delay between E_x and E_y. If $t_{xx} = t_{yy}$ and $\varphi = \pi$, the metasurface can be seen as the half wavelength plate (HWP), where t_{xx}/t_{yy} express the XLP /YLP transmission coefficient, respectively. When the incident light is the circular polarized light, the polarization conversion efficiency can achieve 100%.

For an anisotropic nanobrick structure, there is basically no coupling between the XLP and the YLP light, so$T_{xy} = T_{yx} = 0$; if $t_{xx} = t_{yy}$and$\varphi = \pi$, then, $T_{xx} = -T_{yy}$and anisotropic nanobrick structure can be seen as an HWP. Under the incidence of XLP light, the transmitted field can be expressed as $E_x^t = \begin{bmatrix} T_{xx} & 0 \\ 0 & -T_{xx} \end{bmatrix} \begin{bmatrix} 1 \\ 0 \end{bmatrix} = T_{xx} \begin{bmatrix} 1 \\ 0 \end{bmatrix}$. Under the incidence of YLP light, the transmitted field can be expressed as $E_y^t = \begin{bmatrix} T_{xx} & 0 \\ 0 & -T_{xx} \end{bmatrix} \begin{bmatrix} 0 \\ 1 \end{bmatrix} = -T_{xx} \begin{bmatrix} 0 \\ 1 \end{bmatrix}$. Under the incidence of LCP light, the transmitted field can be expressed as $E_L^t = \begin{bmatrix} 0 & T_{xx} \\ T_{xx} & 0 \end{bmatrix} \begin{bmatrix} 1 \\ i \end{bmatrix} = T_{xx} \begin{bmatrix} 1 \\ i \end{bmatrix}$. Under the incidence of RCP light, the transmitted field can be expressed as $E_R{}^t = \begin{bmatrix} 0 & T_{xx} \\ T_{xx} & 0 \end{bmatrix} \begin{bmatrix} i \\ 1 \end{bmatrix} = T_{xx} \begin{bmatrix} 1 \\ i \end{bmatrix}$. In a word, under the incidence of XLP, YLP, LCP and RCP light, the transmitted field of a HWP can be expressed as

$$E^t = \begin{cases} T_{xx}\vec{e}_{co} & XLP \\ -T_{xx}\vec{e}_{co} & YLP \\ T_{xx}\vec{e}_{cross} & LCP \\ T_{xx}\vec{e}_{cross} & RCP \end{cases} \tag{4}$$

where $\vec{e}_{co}$ is the co-polarization of the incident light, and $\vec{e}_{cross}$is the cross-polarization of the incident light. That is to say, the anisotropic nanobrick structure, whose $t_{xx} = t_{yy}$and $\varphi = \pi$, possesses co-polarization transmission function for XLP and YLP incidences, and possesses cross-polarization transmission function for LCP and RCP incidences, simultaneously. And equation 4 also implies that $t_{xx} = t_{LR} = t_{RL}$,$\phi_{xx} = \phi_{LR} = \phi_{RL}$, where ϕ_{LR} is the phase for the LCP transmission from the incident RCP light, and all of the other elements possess similar definitions, this is an intrinsic characteristics of HWP. It's worth mentioning that the anisotropic nanobrick structure have been researched extensively [43], [44], however, the particular characteristics have not been excavated, and meanwhile the designed metasurface will be polarization-independent, and possess the co-polarized and cross-polarized transmission function for XLP, YLP and CP incidences, respectively.

In order to design a spin-independent HWP with high transmission in the wavelength of 1500 nm, the Si nanobrick adhered to glass substrate is chosen as the basic cell, as shown in Fig. 1(a), the phase accumulation stem from the wave guiding effect proportional to the height, and the height

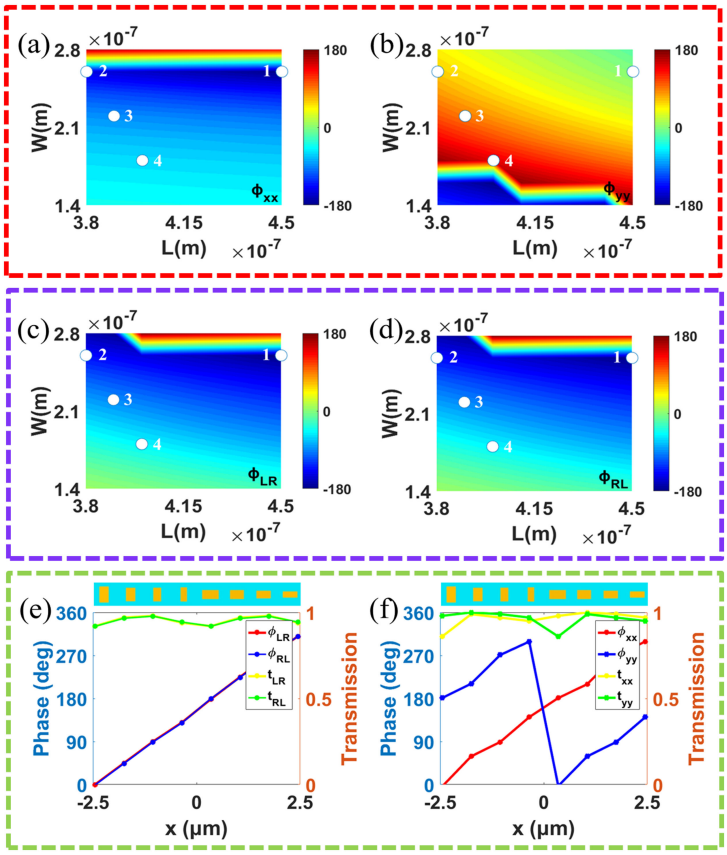

Fig. 2. The phase shift ϕ_{xx}(a), ϕ_{yy} (b), ϕ_{LR} (c), and ϕ_{RL} (d) of the Si nanobrick as a function of length L and width W under the XLP, YLP, LCP, and RCP incidences, respectively. (e) The cross-polarized transmitted amplitudes and phase shifts under LCP and RCP incidences for eight nanobricks. (f) The co-polarized transmitted amplitudes and phase shifts under XLP and YLP incidence for eight nanobricks.

is optimized as 800 nm to realize full 2πphase modulation. The lattice constant P is designed as 700 nm, which is less than half wavelength and can effectively prevent the diffraction. The desired phases of ϕ_{xx}, ϕ_{yy}, ϕ_{LR}, ϕ_{RL} could be obtained through changing the length and width of the Si nanobricks, as shown in Fig. 2(a)–(d). Through simulation analysis based on finite-different time-domain (FDTD) method with the periodic boundary conditions in the x- and y-directions, we selected four nanobricks with the same amplitude and phase difference of almost $\pi/4$, as shown in Fig. 2(a)–(d), there are$\phi_{xx} = \phi_{LR} = \phi_{RL}and\varphi = \pi$for four nanobricks. The structure parameters of four nanobricks are set as $L_1 = 450$ nm, $W_1 = 260$ nm, $L_2 = 380$ nm, $W_2 = 260$ nm, $L_3 = 390$ nm, $W_3 = 220$ nm, $L_4 = 400$ nm, $W_4 = 180$ nm, respectively. The four structures are then rotated 90° counterclockwise to obtain four new nanobricks of equal amplitude and phase increase of π. Above all, the eight nanobricks possess the same transmitted amplitude and phase for LCP and RCP incidences, as shown in Fig. 2(e), so we can say that the metasurface is spin-independent. At the same time, due to $t_{xx} = t_{yy}$ and $\varphi = \pi$of the eight nanobricks, as shown in Fig. 2(f), the metasurface will be HWP with high efficiency and spin independence. It's worth noting that$t_{xx} = t_{LR} = t_{RL}$, $\phi_{xx} = \phi_{LR} = \phi_{RL}$, and the metasurface will have the same optical function for XLP, YLP and CP light. The simulation results agree well with the theoretical analysis, and the proposed intrinsic characteristic of the HWP is also perfectly validated. Meanwhile, we can also say that the metasurface is polarization-independent. However, the polarization-independent principle of the metasurface is completely different from our previous work in which the unit cell itself is polarization-independent [35].

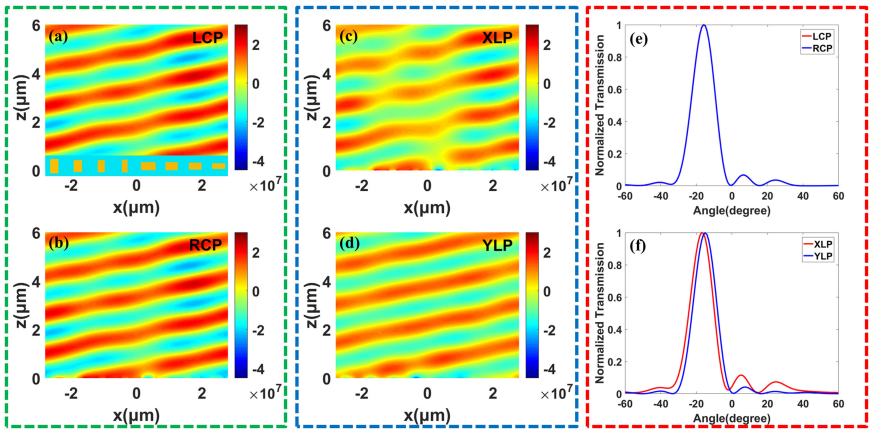

Fig. 3. Transmitted cross-polarized electric field of the beam deflector under LCP (a) and RCP (b) incidence. Transmitted co-polarized electric field of the beam deflector under XLP (c) and YLP (d) incidence. The transmittance as a function of deflection angle under LCP, RCP (e) and XLP, YLP (f) incidence.

To testify our proposed method, firstly, we design a beam polarizer to deflect the CP and LP light into the same directions with high efficiency. As shown in Figs. 2(e) and (f), eight nanobricks can achieve very high cross polarized transmission for CP incidence and co-polarized transmission for XLP and YLP incidences, in which the phase delays are $\pi/4$ between neighbouring unit cells. The overall phases of the eight nanobricks cover $0-2\pi$, which can be used as a supercell of the beam polarizer. As shown in Figs. 3(a, b) and (c, d), the simulated electric fields show that the cross polarized CP and co-polarized XLP and YLP transmission light have been refracted into the same directions. Figs. 3(e) and (f) show the deflection angles are -16°, $-16°$, $-17°$ and $-15°$ for LCP, RCP, XLP and YLP light, respectively, which agree with the theoretical value of $-16°$ based on the generalized Snell's law:$\theta_t = \sin^{-1}(sin\theta_i + \lambda/8P)$. The tiny distinction between XLP and YLP light may be due to the non-symmetrical characteristics of the nanobricks and the setting of the periodic boundary condition, in which periodic boundary condition of unit cell is used along x and y direction, and periodic boundary condition of supercell is used only along y direction. The above phenomena prove our designed beam deflector is polarization-independent for LP and CP incidences.

To testify the feasibility of our design philosophy, we arrange 40 nanobricks to form a cylindrical metalens with a numerical aperture (NA) of 0.86, and the metalens can converge the CP and LP light into the same positions with high efficiency. For CP incidence, the phase shift of the cross-polarized transmitted light should satisfy $\phi(x) = 2\pi/\lambda(\sqrt{x^2 + f^2} - f)$. If the focal length f and wavelength λ is determined, the phase shift at different locations can be determined, in which $f = 8$ μm and $\lambda = 1500$ nm. Due to the special design of the selective eight nanobricks shown in Figs. 2(e) and (f), the metalens will focus the cross-polarized CP and co-polarized XLP and YLP transmission light to the same position. As shown in Figs. 4(a-d), the simulated electric field intensities show that the cross-polarized CP and co-polarized XLP and YLP transmission light possess the same focusing phenomenon, in which the light is well focused at preset position of $f = 8$ μm. The full width at half maximum (FWHM) along the x direction of the focus are 715 nm, 715 nm, 756 nm, 678 nm respectively for LCP, RCP, XLP and YLP incidences, and depth of focus (DOF) are all nearly 2.5 μm respectively for LCP, RCP, XLP and YLP incidences, and the focusing efficiency reach to 73% for CP incidence. These specific data show that the metalens possess the excellent focusing performance for LP and CP light, and further prove that our designed metalens is polarization-independent for LP and CP light.

In order to further verify the reliability and universality of the design method, we also design an optical vortex generator based on the designed metasurface, which can produce vortex beam

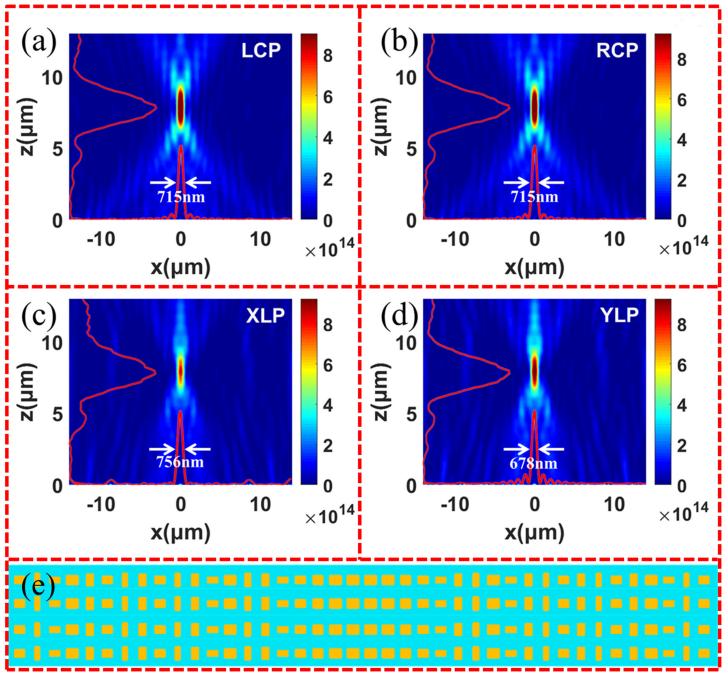

Fig. 4. Simulated intensity distributions of the metalens under LCP (a), RCP (b), XLP (c) and YLP (d) incidence. The red lines indicate the profiles of the FMWHs and DOFs of the focus. (e) The top view of the designed metalens.

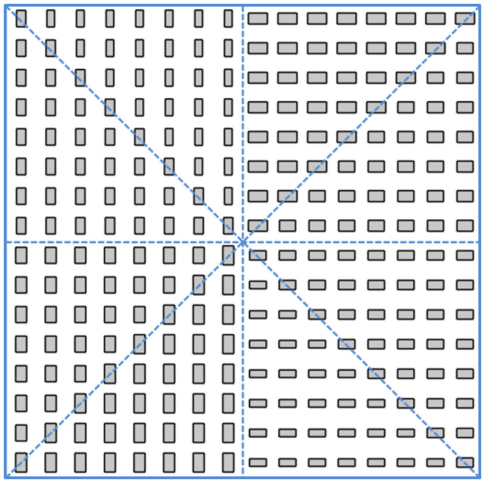

Fig. 5. Schematic of the polarization-independent vortex beam generator.

for CP and LP incidence, as shown in Fig. 5. Based on selected eight spin-dependent nanobrick with $\pi/4$ phase shifts, a vortex beam generator with the topological number $l = 1$ is designed, which is comprised of 16∗16 nanobricks, and eight sectors with $\pi/4$ phase intervals are array incrementally (a phase shift of 2π is realized around the center of the vortex beam generator). The intensity distributions and phase profiles of the cross polarized CP and co-polarized XLP and YLP transmission light are shown in Fig. 6. The wavefront are all counterclockwise for the LCP RCP XLP and YLP incidence light, which means the vortex beam with $l = 1$ have been generated for

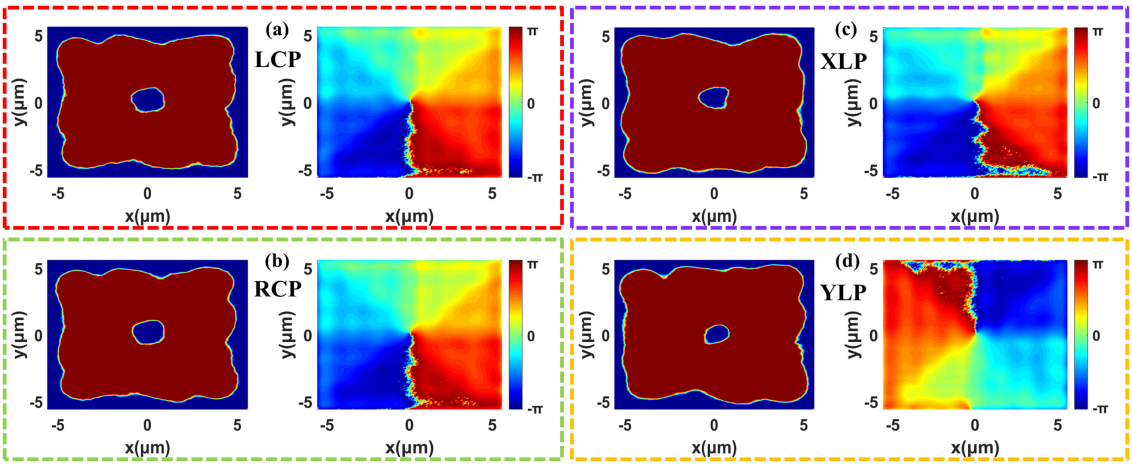

Fig. 6. The intensity and phase distributions of the produced vortex beam under LCP (a), RCP (b), XLP (c), and YLP (d) incidence.

four kinds of polarized incidences. That is to say, the vortex beam generator is also polarization-independent for LP and CP light.

3. Conclusions

In summary, a series of high-efficiency polarization-independent metasurface are demonstrated based on skillfully designed eight irrotational nanobricks with polarization-dependence. The cleverest design for nanobricks is the HWPs that there are the same transmission for cross polarized CP and co-polarized XLP light, and there is a phase difference between XLP and YLP incidences, in which the intrinsic characteristic of the HWP is firstly explored and excavated. Although these nanobricks are polarization-dependent, the metasurface composed of these nanobricks are polarization-independent, and they possess the same transmission function for co-polarized XLP, YLP and cross-polarized CP light. A polarization-independent beam deflector is demonstrated, which can redirect the incident CP and LP lights to an identical refraction angle. A polarization-independent metalens is also demonstrated, which possess the same focusing effect for CP and LP incidences. Finally, a vortex beam generator is demonstrated, which can produce the vortex beam with the same topological number for CP and LP incidence. All these metasurface possess the same function for CP and LP incidences. Our design method can promote strongly the development of polarization-independent metasurface and integrated optics.

References

[1] N. F. Yu *et al.*, "Light propagation with phase discontinuities: Generalized laws of reflection and refraction," *Science*, vol. 334, pp. 333–337, 2011.
[2] N. F. Yu, and F. Capasso, "Flat optics with designer metasurfaces," *Nature Mater.*, vol. 13, no. 2, pp. 139–150, 2014.
[3] X. Ni, N. K. Emani, A. V. Kildishev, A. Boltasseva, and V. M. Shalaev, "Broadband light bending with plasmonic nanoantennas," *Science*, vol. 335, no. 6067, 2012, Art. no. 427.
[4] S.L. Sun *et al.*, "High-efficiency broadband anomalous reflection by gradient meta-surfaces," *Nano Lett.*, vol. 12, pp. 6223–6229, 2012.
[5] A. V. Kildishev, A. Boltasseva, and V. M. Shalaev, "Planar photonics with metasurfaces," *Science*, vol. 339, 2013, Art. no. 1232009.
[6] A. Pors, M. G. Nielsen, R. L. Eriksen, and S. I. Bozhevolnyi, "Broadband focusing flat mirrors based on plasmonic gradient metasurfaces," *Nano Lett.*, vol. 13, pp. 829–834, 2013.
[7] R. Li *et al.*, "Arbitrary focusing metalens by Holographic metasurface," *Photon. Res.*, vol. 3, no. 5, pp. 252–255, 2015.
[8] W. Wang, Z. Zhao, C. Guo, K. Guo, and Z. Guo, "Spin-selected dual-wavelength plasmonic metalenses," *Nanomaterials*, vol. 9, no. 5, 2019, Art. no. E761.

[9] R. Li, F. Shen, Y. Sun, W. Wang, L. Zhu, and Z. Guo, "Broadband, high-efficiency, arbitrary focusing lens by a holographic dielectric meta-reflectarray," *J. Phys. D*, vol. 49, no. 14, 2016, Art. no. 145101.
[10] W. Wang *et al.*, "High-Efficiency and Broadband near-infrared Bi-functional Metasurface based on rotary silicon nanobricks with different sizes," *Nanomaterials*, vol. 9, no. 12, 2019, Art. no. 1744.
[11] H. Zhou, L. Chen, F. Shen, K. Guo, and Z. Guo, "Broadband achromatic metalens in the midinfrared range," *Phys. Rev. App.*, vol. 11, no. 2, 2019, Art. no. 024066.
[12] Z. Guo, L. Tian, F. Shen, H. Zhou, and K. Guo, "Mid-infrared polarization devices based on the double-phase modulating dielectric metasurface," *J. Phys. D*, vol. 50, no. 25, 2017, Art. no. 254001.
[13] K.E. Chong *et al.*, "Polarization-independent silicon metadevices for efficient optical wavefront control," *Nano Lett.*, vol. 15, pp. 5369–5374, 2015.
[14] Z. Guo, L. Zhu, F. Shen, H. Zhou, and R. Gao, "Dielectric metasurface based high-efficiency polarization splitters," *RSC Adv.*, vol. 7, pp. 9872–9879, 2017.
[15] M. Khorasaninejad, W. T. Chen, R. C. Devlin, J. Oh, A. Y. Zhu, and F. Capasso, "Metalenses at visible wavelengths: Diffraction-limited focusing and subwavelength resolution imaging," *Science*, vol. 352, pp. 1190–1194, 2016.
[16] W. Wang, C. Kang, X. Liu, and S. Qu, "Spin-selected and spin-independent dielectric metalenses," *J. Opt.*, vol. 20, 2018, Art. no. 095102.
[17] K. E. Chong *et al.*, "Efficient polarization-insensitive complex wavefront control using huygens' metasurfaces based on dielectric resonant meta-atoms," *ACS Photon.*, vol. 3, pp. 514–519, 2016.
[18] L. Wang *et al.*, "Grayscale transparent metasurface holograms," *Optica*, vol. 3, pp. 1504–1505, 2016.
[19] R. C. Devlin *et al.*, "Spin-to-orbital angular momentum conversion in dielectric metasurfaces: Erratum," *Opt. Express*, vol. 25, no. 4, pp. 377–393, 2017.
[20] H. Zhang *et al.*, "Polarization-independent all-silicon dielectric metasurfaces in the terahertz regime," *Photon. Res.,* vol. 6, no. 1, pp. 24–29, 2018.
[21] T. Cao, L. Zhang, R. E. Simpson, C. Wei, and M. J. Cryan, "Strongly tunable circular dichroism in gammadion chiral phase-change metamaterials," *Opt. Express*, vol. 21, pp. 27841–27851, 2013.
[22] T. Cao, C. Wei, L. Mao, and Y. Li, "Extrinsic 2d chirality: Giant circular conversion dichroism from a metal-dielectric-metal square array," *Sci. Rep.*, vol. 4, 2014, Art. no. 7442.
[23] T. Cao, C. W. Wei, L. B. Mao, and S. Wang, "Tuning of giant 2d-chiroptical response using achiral metasurface integrated with graphene," *Opt. Express*, vol. 23, pp. 18620–18629, 2015.
[24] T. Cao, C. W. Wei, and Y. Li, "Dual-band strong extrinsic 2d chirality in a highly symmetric metal-dielectric-metal achiral metasurface," *Opt. Mater. Express*, vol. 6, pp. 303–311, 2016.
[25] T. Cao, C. Wei, and L. Mao, "Numerical study of achiral phase-change metamaterials for ultrafast tuning of giant circular conversion dichroism," *Sci. Rep.*, vol. 5, 2015, Art. no. 14666.
[26] T. Cao, Y. Li, C. W. Wei, and Y. M. Qiu, "Numerical study of tunable enhanced chirality in multilayer stack achiral phase-change metamaterials," *Opt. Express*, vol. 25, pp. 9911–9925, 2017.
[27] L. L. Huang *et al.*, "Dispersionless phase discontinuities for controlling light propagation," *Nano Lett.*, vol. 12, pp. 5750–5755, 2012.
[28] X. H. Ling, X. X. Zhou, W. X. Shu, H. L. Luo, and S. C. Wen, "Realization of tunable photonic spin hall effect by tailoring the pancharatnam-berry phase," *Sci. Rep.*, vol. 4, 2014, Art. no. 5557.
[29] X. Z. Chen *et al.*, "Dual-polarity plasmonic metalens for visible light," *Nature Commun.*, vol. 3, 2012, Art. no. 1198.
[30] W. Wang *et al.*, "Ultra-thin planar broadband dual-polarity metalens," *Photon. Res.*, vol. 3, pp. 68–71, 2015.
[31] B. Groever, N. A. Rubin, J. P. B. Mueller, R. C. Devlin, and F. Capasso, "High-efficiency chiral meta-lens," *Scientific Rep.*, vol. 8, no. 1, 2018, Art. no. 7240.
[32] M. Khorasaninejad, and K. B. Crozier, "Silicon nanofin grating as a miniature chirality-distinguishing beam-splitter," *Nature Commun.*, vol. 5, 2014, Art. no. 5386.
[33] W. Wang *et al.*, "Ultra-thin optical vortex phase plate based on the metasurface and the angular momentum transformation," *J. Opt.*, vol. 17, no. 4, 2015, Art. no. 045102.
[34] J. W. He, X. K. Wang, D. Hu, J. S. Ye, S. F. Feng, Q. Kan, and Y. Zhang, "Generation and evolution of the terahertz vortex beam," *Opt. Express*, vol. 21, pp. 20230–20239, 2013.
[35] K. Huang *et al.*, "Silicon multi-meta-holograms for the broadband visible light," *Laser Photon. Rev.*, vol. 10, pp. 500–509, 2016.
[36] D. Wen *et al.*, "Helicity multiplexed broadband metasurface holograms," *Nature Commun.*, vol. 6, 2015, Art. no. 8241.
[37] A. Arbabi, Y. Horie, A. J. Ball, M. Bagheri, and A. Faraon, "Subwavelength-thick lenses with high numerical apertures and large efficiency based on high-contrast transmitarrays," *Nature Commun.*, vol. 6, 2015, Art. no. 7069.
[38] M. Khorasaninejad *et al.*, "Polarization-insensitive metalenses at visible wavelengths," *Nano Lett.*, vol. 16, pp. 7229–7234, 2016.
[39] H. F. Zhang *et al.*, "Polarization-independent all-silicon dielectric metasurfaces in the terahertz regime," *Photon. Res.*, vol. 6, no. 1, pp. 24–29, 2018.
[40] Q. T. Li *et al.*, "Polarization-independent and high-efficiency dielectric metasurfaces for visible light," *Opt. Express*, vol. 24, no. 15, 2016, Art. no. 16309.
[41] W. Wang *et al.*, "Polarization-independent characteristics of the metasurfaces with the symmetrical axis's orientation angle of 45° or 135°," *J. Opt.*, vol. 18, no. 3, 2016, Art. no. 035007.
[42] H. Yang *et al.*, "Polarization-independent metalens constructed of antennas without rotational invariance," *Opt. Lett.*, vol. 42, no. 19, pp. 3996–3999, 2017.
[43] J. Wang *et al.*, "High-efficiency terahertz dual-function devices based on the dielectric metasurface," *Superlattices Microstructures*, vol. 120, pp. 759–765, 2018.
[44] Z. Yin *et al.*, "High-efficience dielectric metasurfaces for simultaneously engineering polarization and wavefront," *J. Mater. Chem. C*, vol. 6, pp. 6354–6359, 2018.